AFRL-AFOSR-JP-TR-2018-0020

Development of a Stretchable Tactile Distribution Sensor for Facial Expression-Driven Systems

Norsinnira Azlan
INTERNATIONAL ISLAMIC UNIVERSITY MALAYSIA

03/12/2018
Final Report

DISTRIBUTION A: Distribution approved for public release.

Air Force Research Laboratory
AF Office Of Scientific Research (AFOSR)/ IOA
Arlington, Virginia 22203
Air Force Materiel Command

REPORT DOCUMENTATION PAGE

Form Approved
OMB No. 0704-0188

1. REPORT DATE *(DD-MM-YYYY)*
12-03-2018

2. REPORT TYPE
Final

3. DATES COVERED *(From - To)*
12 Sep 2016 to 29 Sep 2017

4. TITLE AND SUBTITLE
Development of a Stretchable Tactile Distribution Sensor for Facial Expression-Driven Systems

5a. CONTRACT NUMBER

5b. GRANT NUMBER
FA2386-16-1-4040

5c. PROGRAM ELEMENT NUMBER
61102F

6. AUTHOR(S)
Norsinnira Azlan

5d. PROJECT NUMBER

5e. TASK NUMBER

5f. WORK UNIT NUMBER

7. PERFORMING ORGANIZATION NAME(S) AND ADDRESS(ES)
INTERNATIONAL ISLAMIC UNIVERSITY MALAYSIA
JALAN GOMBAK
KUALA LUMPUR, 53100 MY

8. PERFORMING ORGANIZATION REPORT NUMBER

9. SPONSORING/MONITORING AGENCY NAME(S) AND ADDRESS(ES)
AOARD
UNIT 45002
APO AP 96338-5002

10. SPONSOR/MONITOR'S ACRONYM(S)
AFRL/AFOSR IOA

11. SPONSOR/MONITOR'S REPORT NUMBER(S)
AFRL-AFOSR-JP-TR-2018-0020

12. DISTRIBUTION/AVAILABILITY STATEMENT
A DISTRIBUTION UNLIMITED: PB Public Release

13. SUPPLEMENTARY NOTES

14. ABSTRACT
The first year of research focused on the fundamental studies and background research which can be divided into two parts, namely preparation of sensors and implementation of pattern recognition and classification of human facial expressions. For preparation of sensors, a low cost
method of printing sensors using a commercial ink-jet printer was developed and tested. Different designs of the sensors were printed on PET and its sheet resistance were characterized. For the second part, the pattern recognition and classification algorithms were developed and tested using
simulations and experiments.

15. SUBJECT TERMS
biological switching, cognitive sensing, 3D printing biology

16. SECURITY CLASSIFICATION OF: a. REPORT	b. ABSTRACT	c. THIS PAGE	17. LIMITATION OF ABSTRACT	18. NUMBER OF PAGES	19a. NAME OF RESPONSIBLE PERSON
Unclassified	Unclassified	Unclassified	SAR	17	AHLERS, KRISTOPHER

19b. TELEPHONE NUMBER *(Include area code)*
315-227-7009

Standard Form 298 (Rev. 8/98)
Prescribed by ANSI Std. Z39.18

Final Report for AOARD Grant 16IOA040 "Development of a Stretchable Strain Sensor for Facial Expression-Driven Systems"

Date

PI and Co-PI information: **PI:** Anis Nurashikin Nordin; anisnn@iium.edu.my; International Islamic University Malaysia; Department of Electrical and Computer Engineering; Jalan Gombak, 53100, Kuala Lumpur; Phone: 03-61964478; Co-PI: Norsinnira Zainul Azlan; sinnira@iium.edu.my, International Islamic University Malaysia; Department of Mechatronics Engineering; Jalan Gombak, 53100, Kuala Lumpur; Phone: 03-61964456;

Period of Performance: 9/30/2016 – 12/31/2017

Abstract: The first year of research focused on the fundamental studies and background research which can be divided into two parts, namely preparation of sensors and implementation of pattern recognition and classification of human facial expressions. For preparation of sensors, a low cost method of printing sensors using a commercial ink-jet printer was developed and tested. Different designs of the sensors were printed on PET and its sheet resistance were characterized. For the second part, the pattern recognition and classification algorithms were developed and tested using simulations and experiments.

1. Development of Silver Ink-Based Inkjet Printing System for Rapid Prototyping of Electronic Circuits

Introduction:

Recent advances in emerging electronic technologies such as biosensors, wearable electronics, flexible electronics, microelectromechanical systems (MEMS) and the Internet of Things (IoT) spurred the rapid improvements of new and existing on-demand fabrication techniques for electronic circuits. Among these techniques, screen printing and inkjet printing are increasingly popular for rapid prototyping of electronic circuits, due to its relatively low cost and ease of access to fabrication tools. These methods involve the patterning and deposition of conductive material – commonly metal or polymer in paste or colloidal solution – onto a substrate [1]. Screen printing has several obvious advantages for the purposes of circuit fabrication: it is a speedy process for mass production, has many types of printing materials available, and allows multilayered device architectures of different materials. However, screen-printing is not without disadvantages. These include low spatial resolution, relatively high material waste, requiring ad hoc masks for patterning, and operator-dependent reproducibility [2]. For development of proof-of-concepts, these disadvantages increases turnaround time between iterations, and likely involves more optimization work.

Inkjet printing (IJP), at a glance, costs higher due to more expensive colloidal ink, has restricted availability of functional materials, and is a low-speed process at mass production scale. However, IJP makes it up with better spatial resolution, higher repeatability, does not require masks, and consumes much less ink material per square unit of circuitry [2]. Further, IJP is also suitable for depositing both conductive materials and biological materials on substrates in a uniform manner [3]. Current works in this research group uses screen printing for biosensors and flexible electronics fabrication. In addition, we also use Dimatix DMP-2800 research-grade inkjet printing system to experiment on silver-based inkjet-printed electrodes [4]. While research-grade IJP

systems like Dimatix are widely utilized in printed electronics due to its high spatial resolution, reproducibility and versatility of ink and substrate materials [5]–[7], the start-up and maintenance cost is relatively expensive for a commercial equipment. Furthermore, and it requires specialized ink for each type of substrate, and the associated ink usually requires heat-sintering at high temperature [8]. This heat-sintering process adds additional fabrication time, and may affect upstream treatments of any heat-sensitive surface chemistry.
Due to these shortcomings of research-use printers, alternative methods have been explored to exploit the advancements in drop-on-demand printhead technology of consumer printers.
Kawahara and colleagues has developed a low-cost and reliable system for printing silver-based flexible circuits on piezoelectric consumer printers. The team utilized a chemical-sintered, water-based silver nanoparticle (AgNP) ink system and its corresponding substrate developed by Mitsubishi Paper Mills that allows instant circuit patterning and AgNP sintering at room temperature [10]. They have demonstrated using the system to build liquid-level sensors, multi-touch sensors and wearable electronics within several hours of prototyping [11].

This project aims to recreate the silver nanoparticle ink-based inkjet printing system for printed electronics as established by Kawahara and colleagues, and establish baseline performance characteristics of the system within local context, to be referred to for future electronics application. The project also aims to demonstrate system's ability to rapidly prototype biomedical sensors at short turnaround time and low cost.

Experiment:

<u>Materials</u>
Commercial Epson L310 inkjet printer and resin-coated high-quality glossy photo paper. NBSIJ-MU01 silver nanoparticle ink and NB-TP-3GU100 polyethylene terephthalate substrate (PET).

<u>Installation of low-cost silver nanoparticle ink-based electrode printing system</u>
NBSIJ-001 silver nanoparticle ink is loaded into the CYMK ink-tank of an Epson L310 inkjet printer. Ink is pumped from the auxiliary tank into the cartridge through Epson L310 driver's built-in charging function for 20 minutes. Designs are created in AutoCAD 1.5 (Autodesk Inc., San Rafael, CA) or Inkscape 0.91 (open-source available on GitLab, GNU General Public License v2.0), converted into .svg files, and printed onto either photo paper or NB-TP-3GU100 coated PET substrate. Devices printed are cut with scissors to separate from the batch.

<u>Sheet resistance characterization</u>
Squares and rectangles of dimensions of: 1 cm x 1 cm, 2 cm x 1 cm (horizontally and vertically printed), 3 cm x 1 cm (horizontally and vertically printed), 2 cm x 2 cm, 4 cm x 2 cm (horizontal), and 6 cm x 2 cm (horizontal), are printed singly and doubly, in triplicates (each replicate is fabricated separately i.e. in different print queues). Resistivity values are measured end-to-end using Pro'sKit MT-1710 precision multimeter. Sheet resistance values are calculated from:

$$R_s = R_{measured}\left(\frac{W}{L}\right)$$

Where Rs is sheet resistance, Rmeasured is measured resistivity, W is width of electrode (perpendicular to direction of measurement), and L is length of electrode (parallel to direction of measurement).

Resolution characterization
20 mm trace wires are doubly-printed with widths of 100 to 500 μm, in 50 μm increments. End-

to-end resistance are measured. Electrode details are examined using Zeiss Lab.A1 Axio optical microscope (Carl Zeiss Microscopy, Thornwood, NY) at 1000x magnification. For gap study, 1 mm width wires are printed in parallel with gaps 100, 200, 300, 400, 500 and 600 µm in between them. Resistance is measured between adjacent wires, and in concluded to be non-conducting if resistance exceeds 15kΩ. Fabrication and measurements are performed in triplicates.

Results and Discussion:

Installation of low-cost silver nanoparticle ink-based electrode printing system

A silver ink-based fabrication strategy for rapid prototyping of electronic circuits on an office piezoelectric inkjet printer is presented, based on the works by Kawahara et al [11] with slight modifications. An Epson L310 inkjet printer is loaded with NBSIJ-MU01 silver nanoparticle ink, and reliably prints electronic circuits onto its companion coated PET substrate (Figure 1). The total cost of the system consisting of the printer, ink and substrate, at the time of writing, is less than USD550 (MYR2250).

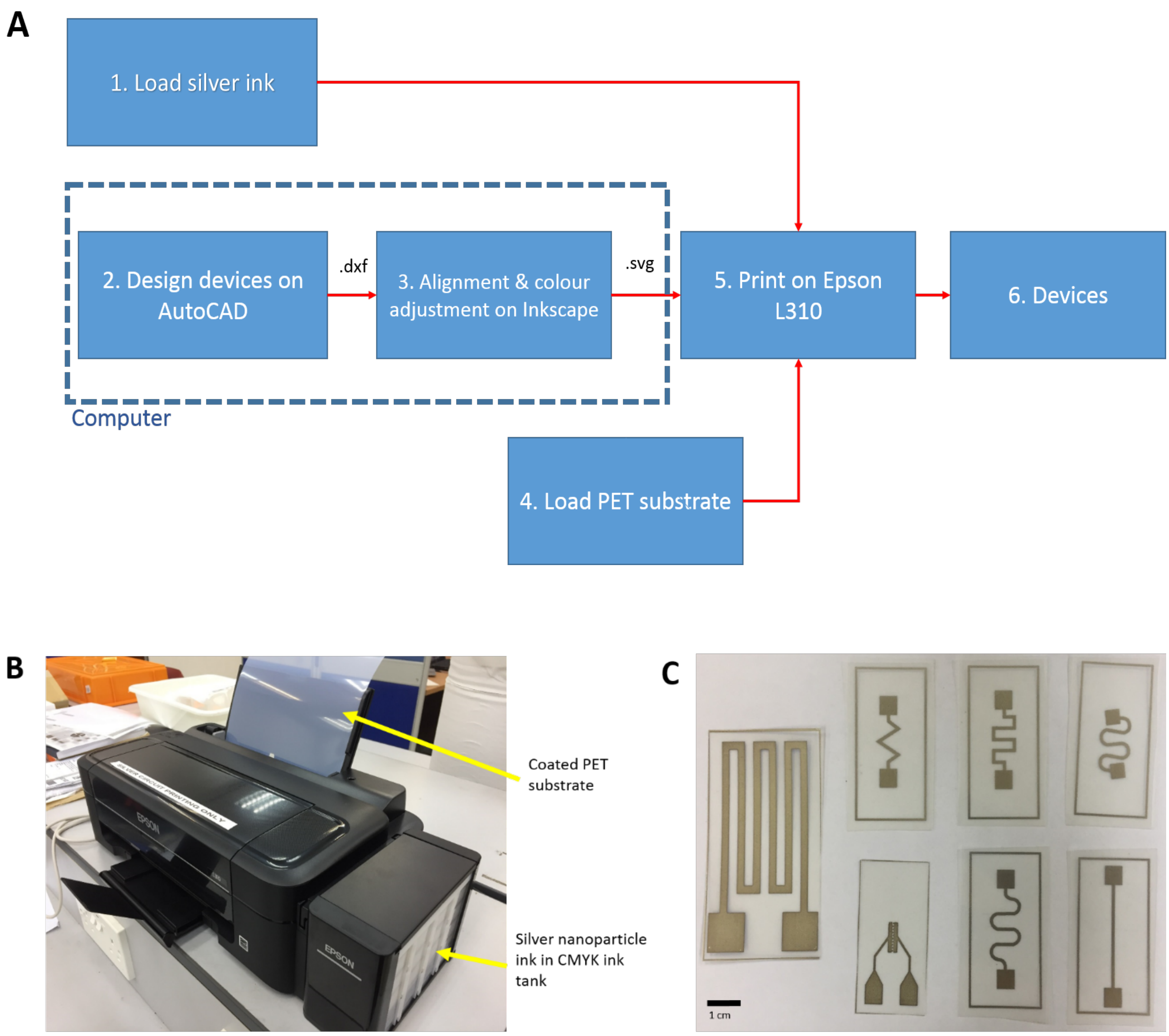

Figure 1. (A) Schematics of the silver inkjet printing process. (B) Silver circuit inkjet printing system. (C) Examples of printed devices.

Effects of substrate, overprinting, and geometry on sheet resistance

Circuits that are printed over the coated PET substrate performs significantly better than the glossy photo paper substrate. Printing similar electrode designs over the substrate multiple times (overprinting) significantly improves its conductivity. To conserve silver ink, it is discouraged to do this more than twice (double-printed). Furthermore, doubly-printed devices are at risk of misalignment of the first printed pattern and the second printed pattern, where features smaller than 200 µm can be lost if poorly aligned.

Sheet resistivity characteristics were measured and recorded as in Table 1. Singly-printed devices are found to potentially have major defects that could render it non-conducting, and conductive devices perform 25 to 37 times worse than doubly-printed devices. Observations under the microscope found that singly-printed devices still have several holes in them, causing dielectric pockets within the device architecture (potentially air, Al2O3-PVA coating, PET, or combination of them).

Interestingly, the geometry of electrodes also plays a significant role in the sheet resistance values. Low aspect ratio features such as squares and rectangles has average sheet resistances around 36 Ω/• for singly-printed, and 980 mΩ/• for doubly-printed patterns. However, high aspect ratio features such as doubly-printed wire traces exhibit Rs values at 280 mΩ/•.

	Sheet resistivity, R_s (Ω/☐)	**Standard deviation (Ω/☐)**
Glossy photo paper		
Singly-printed, average	442 625	104 723
Doubly-printed, average	204 875	7 309
Coated PET substrate		
Singly-printed, average	37.67	35.96
Singly-printed, measured horizontally	19.37	10.09
Singly-printed, measured vertically	65.13	42.21
Doubly-printed, average	0.882	0.388
Doubly-printed, measured horizontally	0.760	0.318

Doubly-printed, measured vertically	1.005	0.267

Table 1. Sheet resistances for different kinds of substrates and numbers of repeated printing. For paper substrate, measurements are done in duplicate on a rectangular pattern with 1:20 aspect ratio. For PET substrate, average values are measured from 6 different low-aspect ratio geometries of squares and rectangles, each fabricated and measured in triplicates. Singly-printed devices may include duplicates and single replicate per geometry to exclude poorly fabricated patterns that are non-conductive (exhibiting $R_s > 100k\Omega$).

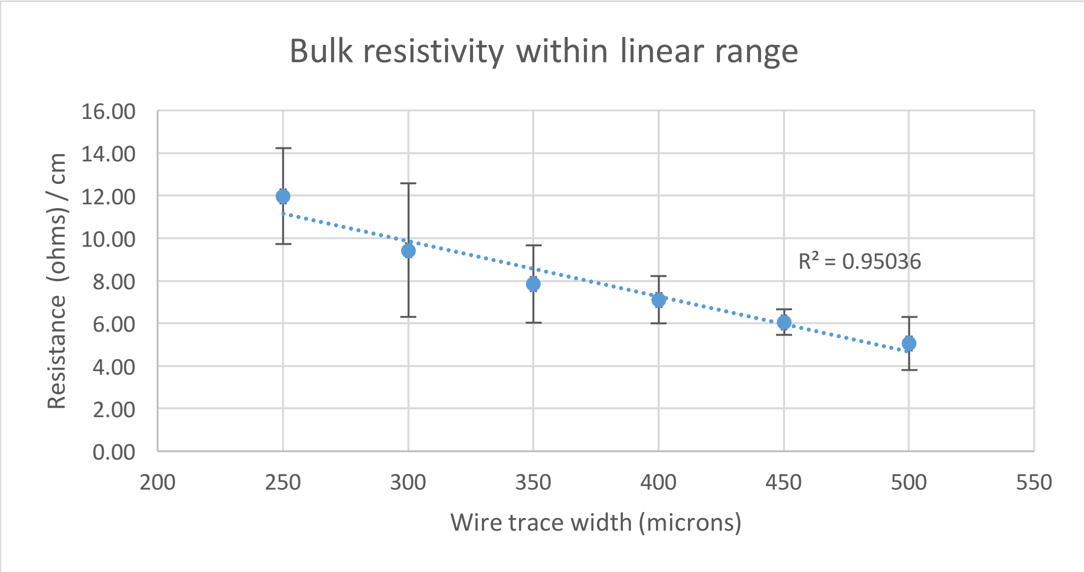

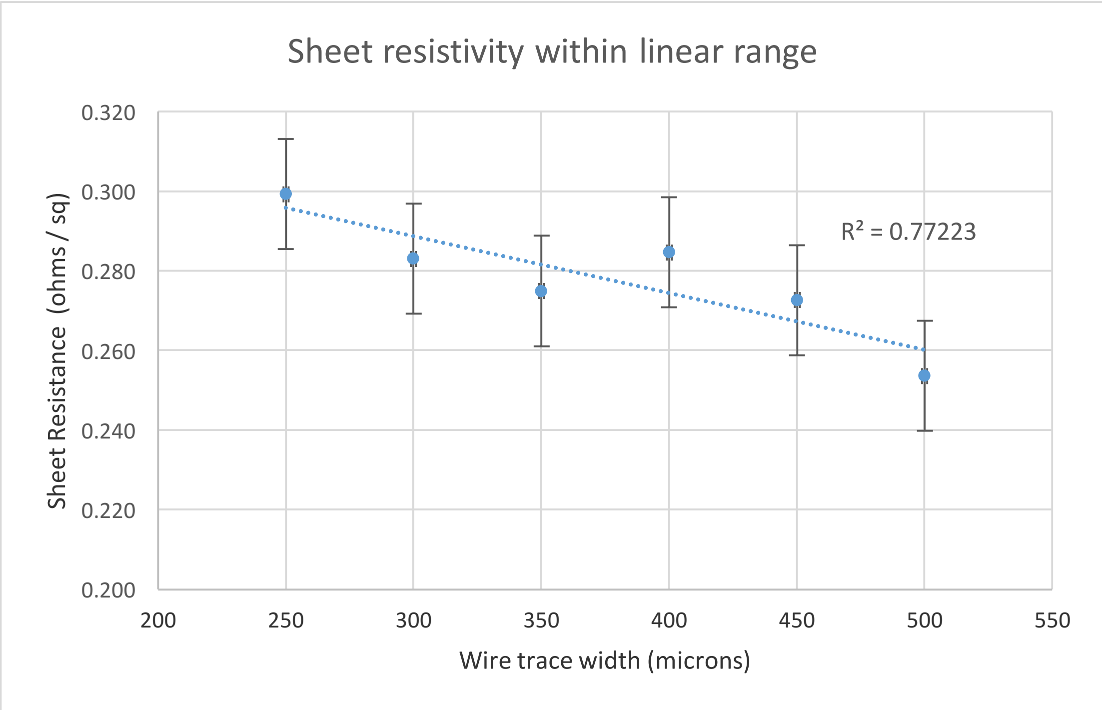

Figure 2. Bulk and sheet resistance curve for wires of lengths 250 µm to 500 µm. Interestingly, while bulk resistance follows a linear decreasing trend, the linearity is

less apparent when sheet resistance are calculated, suggesting that there might be significant batch variations between surface structures of the printed electrodes in range of 250 μm to 500 μm.

Trace and Gap Resolution

A conductivity study across wire traces demonstrates that the minimal width for wires and interdigitated electrode finger that would reliably conduct electricity is 250 μm. End-to-end resistivity measurements for wires of width <250 μm ranges in 1.5 MΩ cm-1 and above, corresponding to sheet resistances of >10kΩ/•. Bulk resistivity at 250 μm is measured at 12 Ω cm-1, and linearly decreases as the width increases. Microscope observation shows that for wires thinner than 250 μm, there can exist several discontinuities on the silver trace (as shown in Figure 3).

For electrical gap study, two adjacent wires are considered distinct if there is sufficiently high resistance between them to determine they are non-conducting. In this study, 15kΩ is arbitrarily chosen as this cut-off. For gap study, 300 μm gaps are the minimum gap size that reliably ensures electrical separation. Microscope observation shows that at the microscale, there might be stray ink blotches seeping from the wires into the gaps. For future works, it might be useful to measure capacitance values across gaps, which we suspect is within the pF range and not measureable with our current instrumentation.

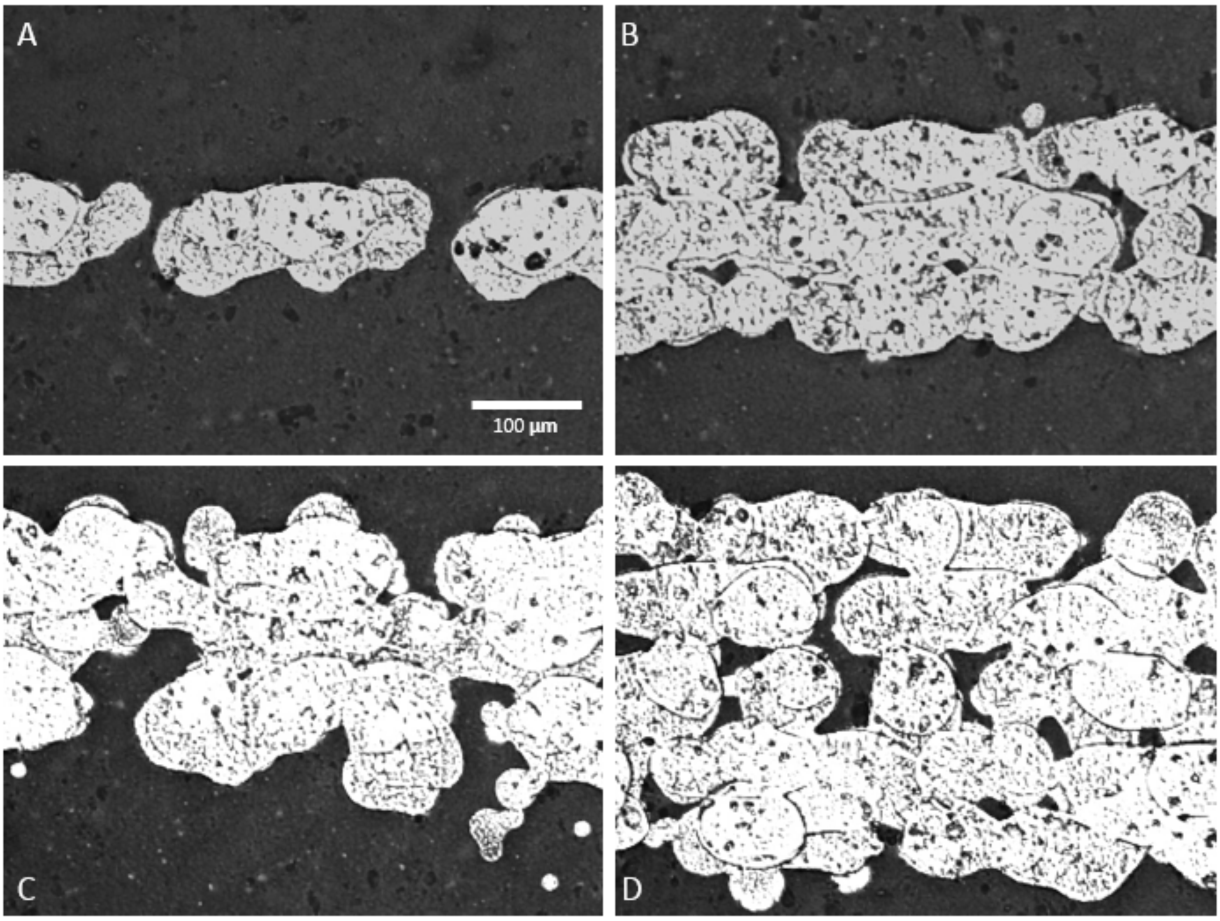

Figure 3. Representative light microscope images of wire traces under 1000x magnification. (A) 100 μm wires, (B) 200 μm wires, (C) 300 μm wires, (D) μm wires.

Note that for 100 µm wires, there exists very noticeable discontinuities within the wire architecture itself.

List of Publications and Significant Collaborations that resulted from your AOARD supported project:

[1] A. N. Nordin and N. Ramli, "Flexible and Stretchable Circuits for Smart Wearables," *J. Telecommun. Electron. Comput. Eng. JTEC*, vol. 9, no. 3–8, pp. 117–122, 2017.

References

[1] S. Khan, L. Lorenzelli, and R. S. Dahiya, "Technologies for printing sensors and electronics over large flexible substrates: A review," IEEE Sens. J., vol. 15, no. 6, pp. 3164–3185, Jun. 2015.

[2] B. Andò, S. Baglio, A. R. Bulsara, T. Emery, V. Marletta, and A. Pistorio, "Low-Cost Inkjet Printing Technology for the Rapid Prototyping of Transducers.," Sensors (Basel)., vol. 17, no. 4, Apr. 2017.

[3] J. Li, F. Rossignol, and J. Macdonald, "Inkjet printing for biosensor fabrication: combining chemistry and technology for advanced manufacturing," Lab Chip, vol. 15, no. 12, pp. 2538–2558, Jun. 2015.

[4] A. A. Zainuddin, A. F. M. Mansor, R. A. Rahim, and A. N. Nordin, "Optimization of printing techniques for electrochemical biosensors," 2017, p. 020066.

[5] D. D. Le, T. N. N. Nguyen, D. C. T. Doan, T. M. D. Dang, and M. C. Dang, "Fabrication of interdigitated electrodes by inkjet printing technology for apllication in ammonia sensing," Adv. Nat. Sci. Nanosci. Nanotechnol., vol. 7, no. 2, p. 025002, Mar. 2016.

[6] P. M. Grubb, H. Subbaraman, S. Park, D. Akinwande, and R. T. Chen, "Inkjet Printing of High Performance Transistors with Micron Order Chemically Set Gaps," Sci. Rep., vol. 7, no. 1, p. 1202, Dec. 2017.

[7] P. H. Bezuidenhout, K. J. Land, and T.-H. Joubert, "Integrating integrated circuit chips on paper substrates using inkjet printed electronics," 2016.

[8] "Silver Jet Ink | Nano-Silver Ink for Inkjet Printing | ANP Co., Ltd." [Online]. Available: http://anapro.com/eng/product/silver_inkjet_ink.html. [Accessed: 19-Sep-2017].

[9] L. Gonzalez-Macia, A. Morrin, M. R. Smyth, and A. J. Killard, "Advanced printing and deposition methodologies for the fabrication of biosensors and biodevices," Analyst, vol. 135, no. 5, pp. 845–867, Apr. 2010.

[10] "Silver Nano | Mitsubishi Paper Mills." [Online]. Available: https://www.mpm.co.jp/electronic/eng/silver-nano/index.html. [Accessed: 19-Sep-2017].

[11] Y. Kawahara, S. Hodges, N.-W. Gong, S. Olberding, and J. Steimle, "Building Functional Prototypes Using Conductive Inkjet Printing," IEEE Pervasive Comput., vol. 13, no. 3, pp. 30–38, Jul. 2014.

[12] K. Nakahara, K. Narumi, R. Niiyama, and Y. Kawahara, "Electric Phase-change Actuator with Inkjet Printed Flexible Circuit for Printable and Integrated Robot Prototyping," 2017.

[13] "Epson Professional Imaging - Color Management Guide."

2. FACIAL EXPRESSION RECOGNITION AND CLASSIFICATION USING STRETCHABLE SENSOR

Introduction:

Human facial expression is the most important and efficient way in exchanging information while communicating and transfer messages. Emotion recognition can be achieved by knowing or studying the position and motion of facial muscles. Facial expression recognition has already been applied for various applications such as retrieval of images and videos, robotics and healthcare.

For humans, facial expression plays an important role to make others understand one's messages. Facial expression is also important for determining the emotional state of a human being.

So far, Feature Method, Biorthogonal Wavelet Entropy and Local Binary Pattern techniques have been used for recognizing the expression.

This project focuses on the pattern recognition and classification of human's facial expression using stretchable sensor. The result of the detection will be used to drive the motion of an existing robotic hand.

Experiment:

Multilayer Feedforward Backpropagation Neural Network algorithm has been used to recognize and classify the output of the stretchable sensors for different facial expression. Each facial expression will activate different motors of a robotic hand and produce separate motions. There are four facial expressions considered in this study, which are

i. Happy
ii. Sad
iii. Normal
iv. Disgust

In the previous study, the stretchable sensors output data for these 4 facial expressions had been collected from 10 subjects which consist of 5 females and 5 males. This is to vary the expressions data for different people. The sensors have been placed at the forehead, upper lip, lower lip and left cheek. These four specific positions have been chosen as they show the most obvious changes with respect to different expression.

The feature of the data has been extracted under four criteria, which are

i. Mean
ii. Root Mean Square(RMS)
iii. Variance (Var)
iv. Standard Deviation (STD).

Training and testing have been conducted using Neural Network Toolbox in MATLAB to train and test the feasibility of the algorithm in recognizing and classifying the human expression. In this process, the extracted input data which had been collected from 8 subjects in the previous study were used for training purpose and the data from 2 other subjects were utilised for testing purpose. The training data had been arranged into 16 x 32 matrix, where the 16 rows represent the 4 different criteria from 4 stretchable sensors including the mean, rms, variance and standard deviation, while the 32 columns represent 4 facial expressions for 8 subjects. Similarly the testing data had been set as 16 x 8 matrix where the 8 columns denotes the criteria values for 2 subjects under 4 different facial expressions.

The values of the target or output for training and testing processes had been assigned as in Table 2.1.

Table 2.1 Output Setting

Facial Expression	Output 1	Output 2
Normal	0	0
Happy	0	1
Sad	1	0
Disgust	1	1

Figure 2.1 shows the drawing of the robotic hand and its position at rest position. The connection of each fingers to the motors are as below

i. Finger 1 is connected to servo 1 which is represented by the orange line.
ii. Finger 2 and 3 are connected to servo 2 which is represented by the green line.
iii. Finger 3 and 4 are connected to servo 3 which is represented by the blue line.
iv. The hand is connected to servo 4 which is located at the bottom of the hand.

The respective servo motor will be activated depending on the output of the facial expression classification to produce different hand gesture as summarized in Table 2.2. The flowchart of the operation of the facial expression driven robotic hand is described in Fig. 2.2.

Table 2.2 Activated servo motor and robotic hand gesture

Facial Expression	Output 1	Output 2	Servo Motor Activated	Robotic Hand Gesture
Normal	0	0	Servo 1, Servo 3	“Peace”
Happy	0	1	Servo 2, Servo 3	“Thumbs up”
Sad	1	0	Servo 1, Servo 2, Servo 3	“Fist”
Disgust	1	1	Servo 4	Hand rotates 180°

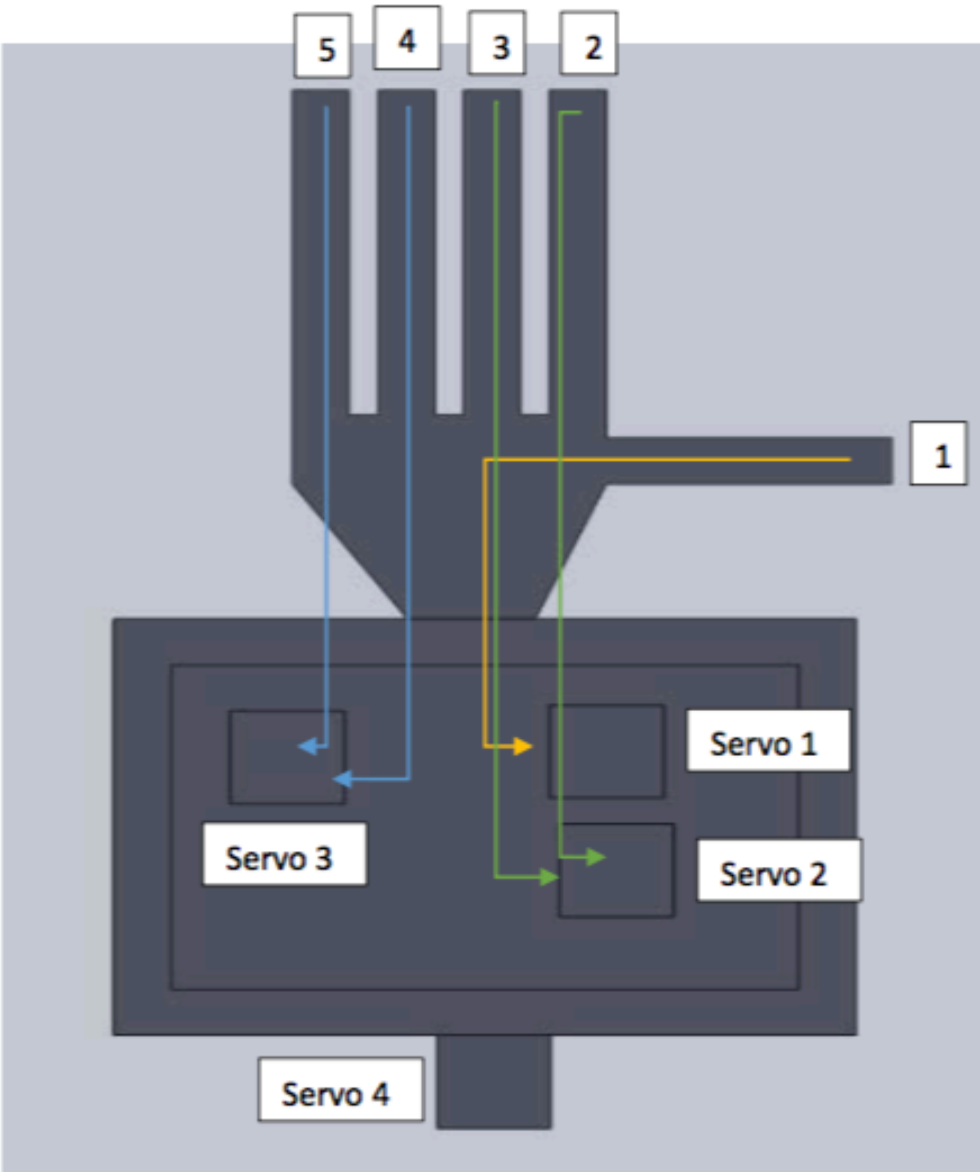

Fig. 2.1 Robotic hand configuration

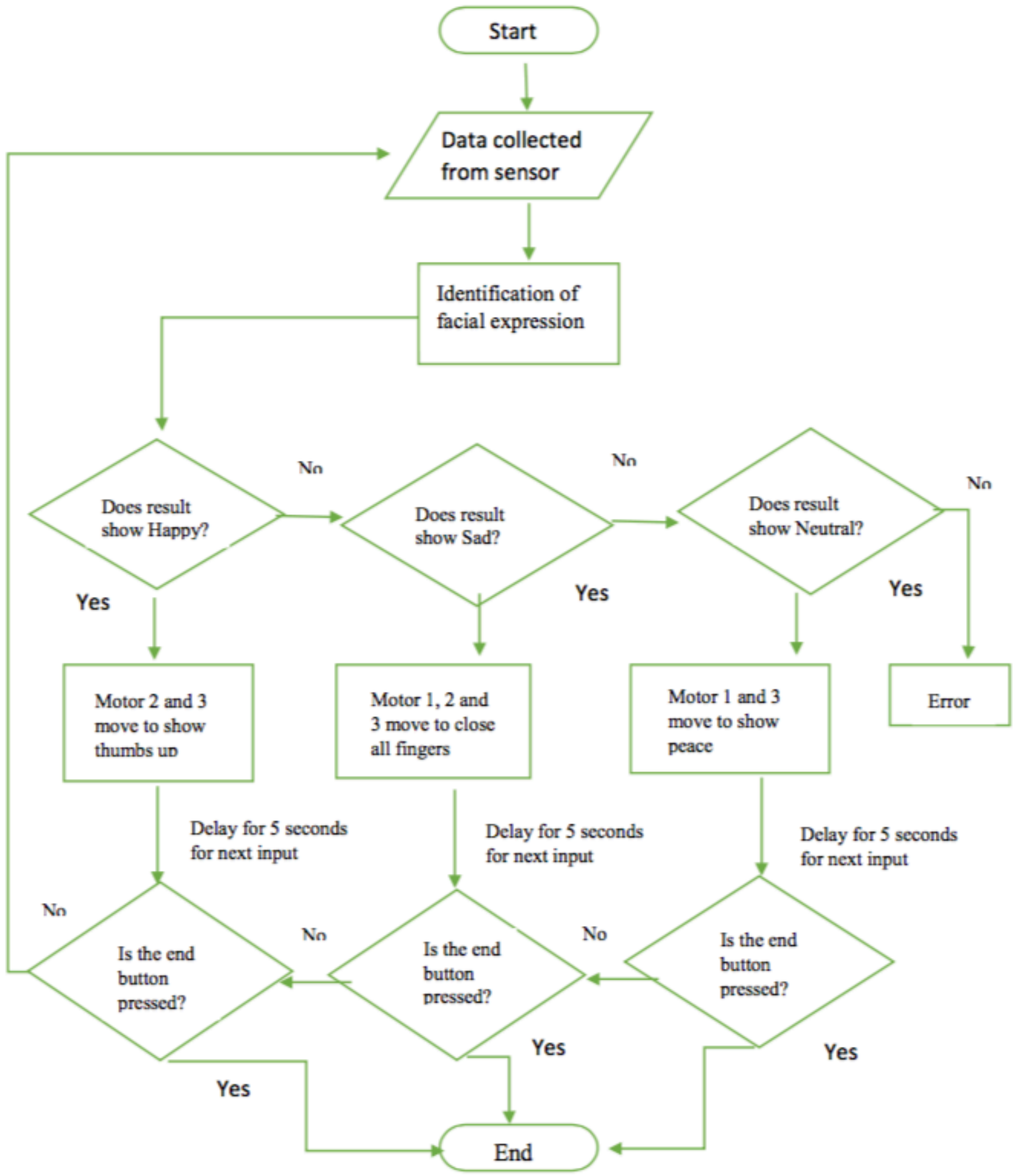

Fig. 2.2 Flowchart of the facial expression driven robotic hand

Results and Discussion:

A sample of the stretchable sensor measurements recorded for "Happy" expression is illustrated in Figure 2.3. Figure 2.4 show the steps implemented in MATLAB to train the neural network including the neural network setting display, network arrangement, training data setting and network training setting.

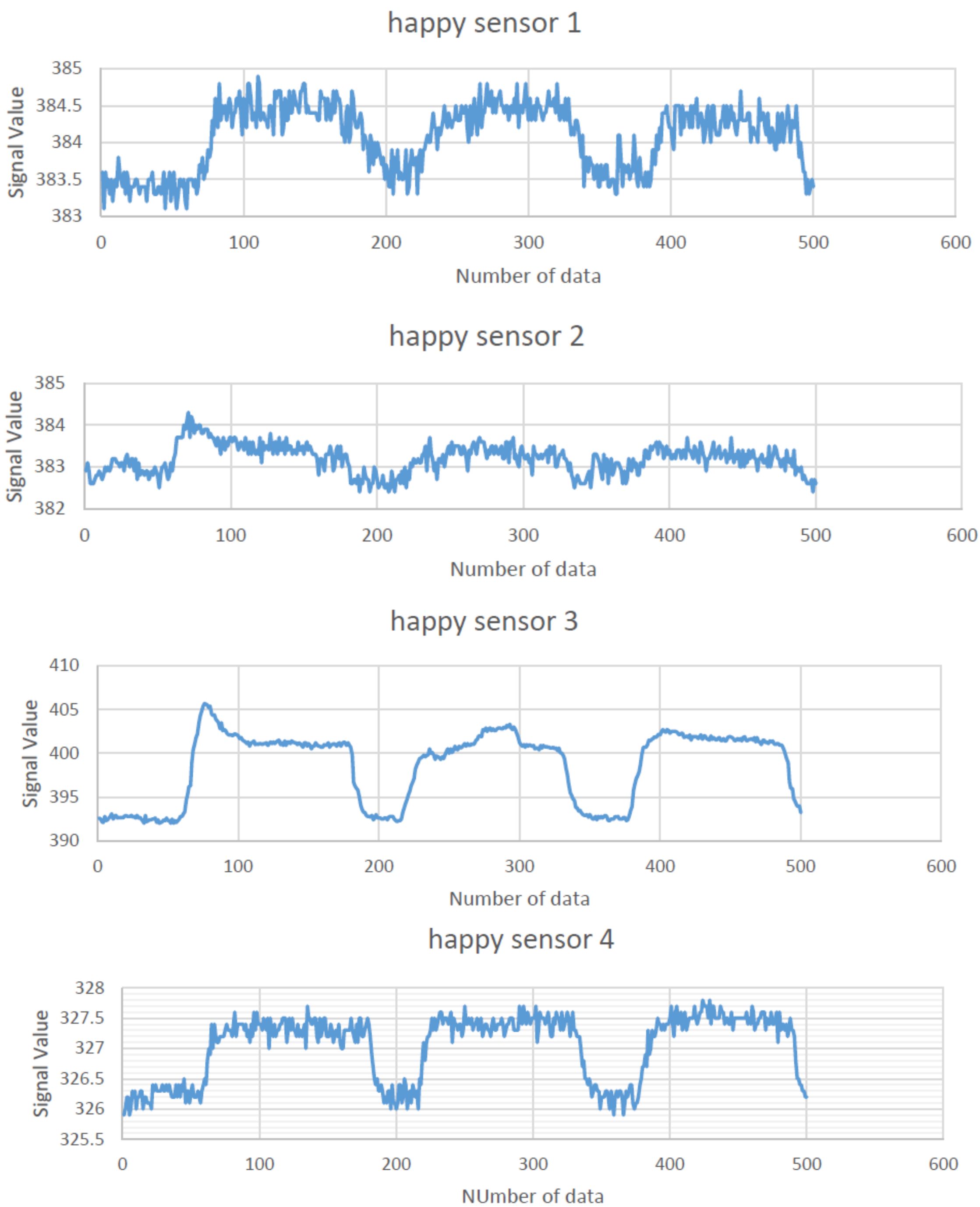

Figure 2.3 Sample of stretchable sensor output signal for happy expression

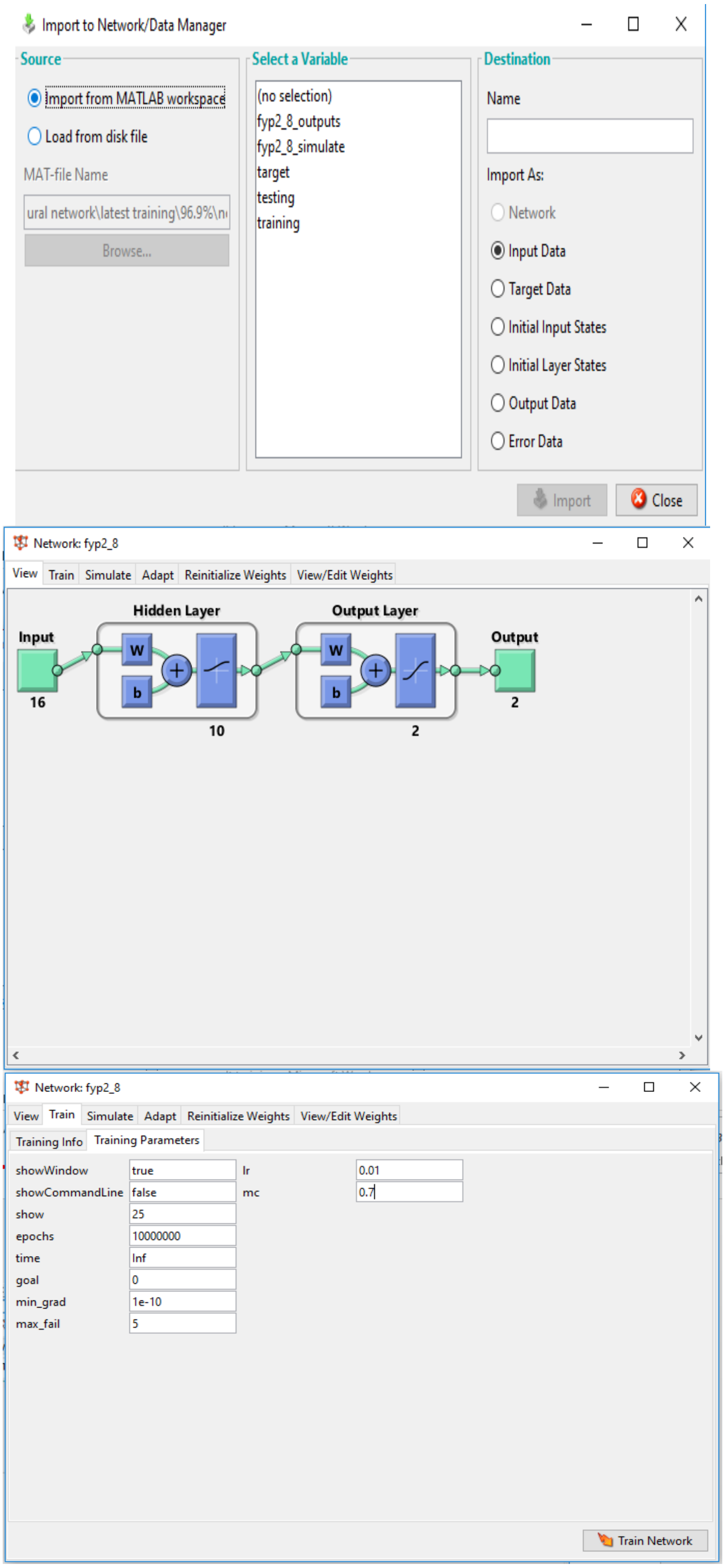

Figure 2.4 Matlab setting for neural network training

First, the trained network has been tested using training data set for 2 random subjects. Table 2.3 shows the output of the test. In this result, any output value that is less than 0.5 is considered as “0” and the output value that is equal or greater than 0.5 is considered as “1”. Therefore, the equivalent output assignment for the result can be depicted as in Table 2.4.

The success rate or performance of the Artificial Neural Network (ANN) in identifying the facial expression can be calculated by

$$\text{ANN Performance} = \frac{number\ of\ correct\ pattern\ recognised}{total\ number\ of\ patterns} \text{ x } 100\% \qquad (2.1)$$

Comparing the results obtained in Table 2.4 with the output assignment in Table 2.1, and utilizing Eq. (2.1), the performance of the neural network has been calculated to be 100%. From this test, it can be seen that the trained neural network can classify all the 8 facial expressions correctly.

Table 2.3 Test results using training data sets

	S1	S2	S3	S4	S5	S6	S7	S8
	NORMAL	HAPPY	SAD	DISGUST	NORMAL	SAD	DISGUST	SAD
OUT_1	0.047789	0.244395	0.987641	0.921924	0.211337	0.664138	0.941253	0.941124
OUT_2	0.027911	0.976811	0.062829	0.993586	0.043519	0.234682	0.982698	0.029577

Table 2.4 Equivalent output assignment of the test results using training data sets

	S1	S2	S3	S4	S5	S6	S7	S8
	NORMAL	HAPPY	SAD	DISGUST	NORMAL	SAD	DISGUST	SAD
OUT_1	0	0	1	1	0	1	1	1
OUT_2	0	1	0	1	0	0	1	0

The test has been repeated using of the testing data sets from the remaining 2 subjects. Tables 2.5 and 2.6 show the output of the test and the equivalent output assignment respectively. From the result, the ANN performance has been calculated to be 25% where 2 expressions are classified correctly by the network. This may be resulted due to insufficient training data or features extracted for the training. It has also been observed that high number of training data will cause a long training duration. Therefore. a further study need to be conducted to increase the performance and success rate of the algorithm, and to reduce the training time.

Table 2.5 Test results using testing data sets

	S1	S2	S3	S4	S5	S6	S7	S8
	HAPPY	SAD	NORMAL	DISGUST	NORMAL	DISGUST	SAD	HAPPY
OUT_1	0.926338	0.999987	0.416627	0.592372	1	0.999972	0.980959	0.999998
OUT_2	0.700746	0.998943	0.129491	0.34886	0.011539	1	0.990425	0.999994

Table 2.6 Equivalent output assignment of the test results using testing data sets

	S1	S2	S3	S4	S5	S6	S7	S8
	HAPPY	SAD	NORMAL	DISGUST	NORMAL	DISGUST	SAD	HAPPY
OUT_1	1	1	0	0	1	1	1	1
OUT_2	1	1	0	0	0	1	1	1

Figure 2.5 show the resulted hand robotic configuration under different facial expression.

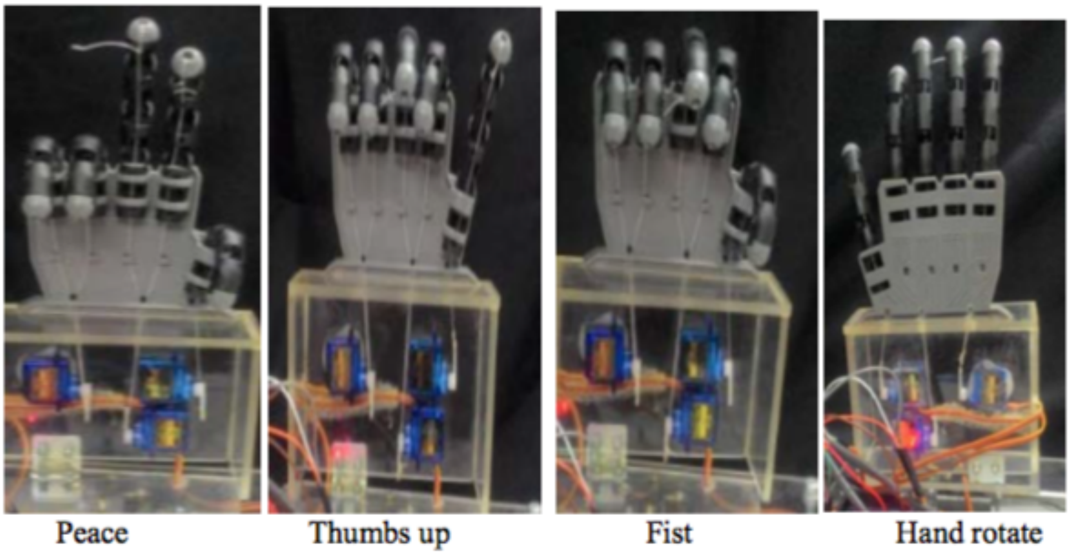

Fig. 2.5 Robotic hand outputs under different facial expressions

List of Publications and Significant Collaborations that resulted from your AOARD supported project:

Due to the short duration (1 year) of the report all manuscripts are currently in preparation